

# Aging after shear rejuvenation in a soft glassy colloidal suspension: evidence for two different regimes

F. Ianni<sup>1,2,\*</sup>, R. Di Leonardo<sup>2</sup>, S. Gentilini<sup>1</sup>, and G. Ruocco<sup>1,2</sup>

<sup>1</sup> Dipartimento di Fisica, Università di Roma “La Sapienza”, I-00185, Roma, Italy.

<sup>2</sup> SOFT-INFN-CNR c/o Università di Roma “La Sapienza”, I-00185, Roma, Italy.

(Dated: April 16, 2018)

The aging dynamics after shear rejuvenation in a glassy, charged clay suspension have been investigated through dynamic light scattering (DLS). Two different aging regimes are observed: one is attained if the sample is rejuvenated before its gelation and one after the rejuvenation of the gelled sample. In the first regime, the application of shear fully rejuvenates the sample, as the system dynamics soon after shear cessation follow the same aging evolution characteristic of normal aging. In the second regime, aging proceeds very fast after shear rejuvenation, and classical DLS cannot be used. An original protocol to measure an ensemble averaged intensity correlation function is proposed and its consistency with classical DLS is verified. The fast aging dynamics of rejuvenated gelled samples exhibit a power law dependence of the slow relaxation time on the waiting time.

## INTRODUCTION

Soft glassy colloidal suspensions are widespread in nature and are of broad technological importance. Macroscopically, they are characterized by a non-Newtonian rheology and, often, by a viscosity that increases many orders of magnitude as time evolves and the gelation process proceeds [1]. These complex fluids also exhibit a strong sensitivity to external forces and have mechanical properties typical of soft solids, such as solid-like behavior below a finite yield stress and thixotropic response to applied deformation [2]. In particular, a shear flow may induce a thinning effect and reduce the fluid viscosity. At the microscopic level, the gelation process corresponds to a slowing down of the structural relaxation with the elapsed time: such a behavior is called aging. Moreover, the system structural dynamics are accelerated by the shear flow. This phenomenon is called shear rejuvenation. The competition between the thickening, produced by the aging, and the thinning, induced by shear flow, gives rise to interesting phenomena.

On the theoretical and numerical side, evidences of the competition between these two effects come from the extension of slow dynamics theories in complex systems, such as mode coupling theory (MCT) [3], mean-field models [4], trap models [1] and molecular dynamics simulations [5, 6, 7], to the presence of external driving forces. These studies show that the structural dynamics are very sensitive to even moderate shear rates, providing that the characteristic timescale for structural rearrangements becomes of the same order of the inverse shear rate. In particular, even starting from non equilibrium, aging states, the presence of shear ensures the existence of a stationary state whose correlation function decays to zero on a timescale given by  $\dot{\gamma}^{-1}$ .

On the experimental side, the investigation of the shear-influenced slow dynamics at the microscopic level is still relatively poor. Diffusing Wave Spectroscopy (DWS) [8, 9, 10] and Light Scattering Echo (LSE) experiments

[11, 12] gave indirect evidences for a shear dependent structural relaxation time and for rejuvenation of aged samples. Unfortunately, the statistical properties of multiple scattered light (probed in DWS and LSE experiments) are not easily represented in terms of the particles’ correlation functions, which, on the contrary, is the outcome of the dynamic light scattering technique in the single scattering regime (DLS). The DLS technique probes the intermediate scattering function of the colloidal particles  $F_q(t)$  [13], which plays a central role in both theoretical and numerical approaches. The intermediate scattering function of a colloidal suspension exhibits two decays: a fast relaxation, which accounts for single particle diffusion, and a slow relaxation, whose characteristic timescale  $\tau_s$  grows many orders of magnitude with the waiting time  $t_w$  and accounts for the structural rearrangements of the system. At long  $t_w$  the system enters a glass or gel phase; only the fast relaxation remains and is observed as a decay towards a plateau, reflecting the onset of structural arrest.

Unfortunately, also DLS suffers of limitations. Indeed, it is not the proper technique to investigate the system dynamics when the characteristic slow relaxation time  $\tau_s$  becomes very large or the aging dynamics proceed very fast. The correlation function is usually measured as an average on the time origin and the experimental acquisition time needed to get a good signal to noise ratio must be kept longer than  $\tau_s$  and shorter than the time one should wait before changes in  $\tau_s$  are significant. On the contrary, Multi-Speckle Dynamic Light Scattering (MS-DLS) or Multi-Speckle Diffusive Wave Spectroscopy (MS-DWS) perform an ensemble average over the speckle pattern of the light scattered intensity and acquisition time is strongly reduced. This enables the investigation of the system dynamics for much longer waiting times  $t_w$  or for faster aging processes. However, in both techniques, the time resolution is much smaller than in DLS, as it is limited by the camera device used as detector. Overall, the experimental studies of aging and rejuvenation

nation under shear of colloidal suspensions still suffer of technical limitations and the "ideal" technique has not yet been introduced.

On the samples' side, among others, proper candidates for the study of the aging and rejuvenation phenomena in soft glassy colloids are suspensions of charged anisotropic colloidal particles such as clay, which have been widely investigated both for their important industrial application [15] and as a prototype of soft glassy materials [16, 17, 18, 19]. Screened charged interactions between these anisotropic particles induce the formation of disordered arrested phase in the suspension even at very low volume fractions [17]. In particular, for sufficiently concentrated samples, a two stage aging process has been observed through DLS experiments in a Laponite sample, a suspension of 25 nm diameter discoidal charged particles [20]: for small  $t_w$ , the structural relaxation time  $\tau$  increases exponentially, or more than exponentially, with  $t_w$ , while for long  $t_w$ , when  $\tau > t_w$ , a power law behavior shows up. The rejuvenation effect of a shear flow on such systems has been investigated using DWS [8, 10], LSE [12], and DLS [21]. The particles' dimension, the sample's history and the kind of shear applied vary among these works; consequently, the effects of the rejuvenation on the aging dynamics changes and a comprehensive picture of the phenomenology has not yet been reached. In Ref. [21], a Laponite suspension is used and the waiting time is set to zero after the sample filtration. Normal aging in such a sample is characterized by an intermediate scattering function having a stretched exponential slow relaxation, whose characteristic time  $\tau_s$  grows exponentially with waiting time  $t_w$  while becoming strongly stretched. Moreover, an exponential relaxation process is observed at short times and its characteristic time  $\tau_f$  slightly increases with  $t_w$  [22]. To investigate the evolution of the aging dynamics during a steady shear, measurements are acquired while the shear is stopped for a few minutes between different shearing periods. The system dynamics soon after shear cessation are affected by the shear flow just applied. In particular, they are characterized by a strong reduction of aging as soon as  $\tau_s$  enters the timescale set by the inverse shear rate. In [10, 12], aged samples of Saponite particles, 125 nm diameter charged platelets, are rejuvenated by a strong oscillating shear, after which the counting of  $t_w$  starts. The sample is then submitted to various periodic shear protocols and dynamics of tracer particles are investigated during shear and after shear cessation. Under these conditions, aging is much faster and the structural relaxation time exhibits a power law dependence on  $t_w$ . In this paper, we aim to elucidate the apparently contrasting behavior observed in the two previously described systems [21, 22] and [10, 12]. We investigate an aqueous suspension of Laponite, a synthetic layered silicate composed of monodisperse discoidal particles, which get charged in water. Aging dynamics following the shear

rejuvenation before the sample gelation occurs are investigated through DLS technique. On the contrary, aging after rejuvenation of gelled samples is very fast and classical DLS could not be used, as the system wouldn't be stationary during the acquisition time. Thus, a novel protocol of DLS acquisition, consisting in an ensemble average over many rejuvenating experiments, is proposed to measure the intensity correlation function and its coherence with classical DLS is checked. This new method has the double advantage of probing the intermediate scattering function of the colloidal particles as in classical DLS, with the "ensemble" average enabling the investigation of a dynamics changing very rapidly in the system, while a time resolution much higher than in MS-DLS technique is achieved. As a result, we find the existence of two different regimes of aging after shear rejuvenation as a common feature of charged discoidal clay suspensions. If the shear is applied before sample gelation is completed, the rejuvenation is followed by a slow aging regime, behaving just like normal aging after sample preparation. On the contrary, when a gelled sample is rejuvenated by shear, we observe a fast aging regime after the shear cessation, characterized by a power law dependence of the slow relaxation time on the waiting time.

## EXPERIMENTS AND RESULTS

The investigated system consists of an aqueous suspension of Laponite RD, a synthetic layered silicate provided by Laporte Ltd. Particles are disk shaped with a diameter of 25 nm and 1 nm thickness. Laponite powder is dispersed in ultrapure water at 3% wt concentration and stirred for  $\sim 30$  min. The obtained suspension, which is optically transparent and initially "liquid", is loaded into a home made, cone and plate shear cell having a flat optical window as the static plate. Cell loading (through a 0.45  $\mu\text{m}$  filter) is taken as the origin of waiting times for normal aging. Incident laser beam (diode pumped solid-state laser,  $\lambda = 532$  nm,  $P = 150$  mW) and scattered light pass through the same optical window. The scattered light is collected by a mono-mode optical fiber and detected by a photomultiplier, after being optionally mixed with a coherent local oscillator field. Photocounts are acquired through a general purpose, counter/timer PCI board (National Instruments PCI 6602). We developed a set of software classes (implemented as extension modules of the object oriented language Python) designed to perform basic tasks for the statistical analysis of digital pulse trains. A typical application is real time multi-tau photon correlation. However, a software approach, having access to the full photocounts train, allows to efficiently prototype different analysis protocols, going far beyond the simple autocorrelation function [23]. The scattering geometry is fixed (scattering vector  $q = 22 \mu\text{m}^{-1}$ ). The shift of the cell allows us to

select the position of the scattering volume in the cell gap and the possibility of choosing an heterodyne correlation scheme [24] enables direct access to the detailed velocity profile in the shear cell.

### Rejuvenation before gelation

We first investigate the aging dynamics that follows a shear rejuvenation induced before the full gelation of the sample takes place. We let the system age for a time  $t_w^0$  after cell loading, then we apply a shear and finally we follow the dynamics after shear cessation through DLS. We define  $t_w$  the time elapsed since shear cessation. Aging of the system is monitored through the normalized intensity autocorrelation function  $g^{(2)}(t_w, t) = \langle I(q, t_w) I(q, t_w + t) \rangle_T / \langle I(q, t_w) \rangle_T^2$ , where  $\langle \dots \rangle_T$  indicates temporal average over the acquisition time  $T$ . In the single scattering regime and within the Gaussian approximation  $g^{(2)}(t_w, t) = 1 + |F_q(t_w, t)|^2$  [13], where  $F_q(t_w, t) = \langle \rho_{-q}(t_w) \rho_q(t_w + t) \rangle / \langle \rho_{-q}(t_w) \rho_q(t_w) \rangle$  is the intermediate scattering function of the colloidal particles. An example of the results of this procedure is reported in Fig. 1, left panel. In this example, at  $t_w^0 = 13.4$  h a shear rate of  $100 \text{ s}^{-1}$  is applied for two minutes; once the shear is stopped, aging is followed through the intensity autocorrelation function  $g^{(2)}(t_w, t)$  for a set of  $t_w$  between 0.2 and 3 hours. As for normal aging, the two step decay for  $F_q(t_w, t)$ :

$$F_q(t_w, t) = f \exp[-(t/\tau_s)^\beta] + (1-f) \exp[-t/\tau_f] \quad (1)$$

where all parameters ( $f$ ,  $\tau_s$ ,  $\beta$ ,  $\tau_f$ ) depend on  $t_w$ , provides a very good fit for all the correlations. As the waiting time  $t_w$  evolves, the slow relaxation decay becomes more stretched: the stretching parameter  $\beta$  is smaller than one and decreases with  $t_w$ , as shown in the left panel of Fig. 2. In order to quantify the slow decay timescale, we calculate the average slow relaxation time  $\langle \tau_s \rangle$  ( $\langle \tau_s \rangle = \int_0^\infty \exp[-(t/\tau_s)^\beta] dt = \tau_s / \beta \Gamma(1/\beta)$ , where  $\Gamma$  is the Euler Gamma function) and we plot it as a function of  $t_w$  in Fig. 3 (full circles). The evolution of  $\langle \tau_s \rangle$  as a function of  $t_w^0$  for the normal aging is also plotted (open circles). In order to show that shear application completely rejuvenates the system, the  $t_w$  axis for aging after shear rejuvenation has been shifted by superimposing the first point of the curve on the normal aging curve. The same behavior can be observed in the evolution of the fast relaxation timescale  $\tau_f$ , which is plotted in the inset of Fig. 3. In fact, the dependence of the fast relaxation time on the waiting time is in disagreement with previous observations [19, 20], that assigned the fast dynamics to the single particle diffusion.

Summarizing, once a shear is applied before gelation, a reduced timescale for relaxation is observed soon after shear stops. This starting value depends on the applied shear rate, as evidenced in Ref. [21]. The following

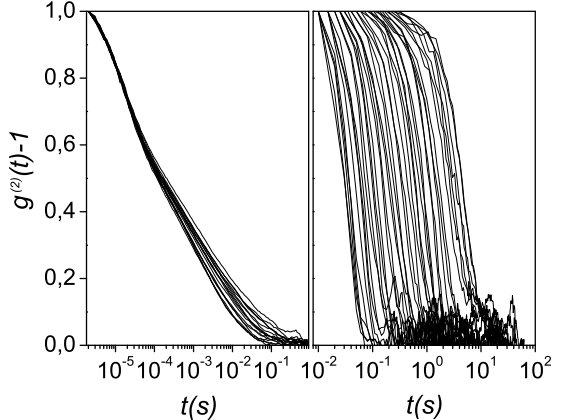


FIG. 1: Normalized intensity autocorrelation functions for two different aging regimes after shear rejuvenation. *Left*: a Laponite sample rejuvenated before entering the arrested phase. Correlation functions are obtained from an average on the time origin for 16 equally spaced waiting times between 0.2 and 3 hours (from left to right) after shear cessation. *Right*: a gelled Laponite sample for a set of waiting times between 0.3 s and 40 s (from left to right) after shear cessation. Correlation functions are obtained from an ensemble average over bunches of counts, all acquired after the application of the same shear rate for a duration of two minutes.

evolution of the relaxation times (both fast and slow) traces the same aging curves (once the waiting time axis is shifted) exhibited during normal aging, showing that complete rejuvenation is achieved through shear flow.

### Rejuvenation after gelation

We now turn to the investigation of the aging evolution after a shear is applied to gelled samples. Before describing the measurements in such a regime, we want to point out that when the gelled Laponite suspension is put under shear, drastic wall slip takes place and all the fluid rotates as a solid body leaving a null shear in the core. Measurements of the velocity profile are performed through the heterodyne dynamic light scattering setup [24]. In order to apply a controlled shear to rejuvenate the gelled sample, the solid band is first broken through the application of a high shear rate ( $\dot{\gamma}_0 > 100 \text{ s}^{-1}$ ) of the duration of two minutes. We checked that this strong shear doesn't alter the nature of aging dynamics after subsequent shear applications. In such a regime, the sample is found to quickly age back to a gel state. By looking at the intensity scattered by the sample after shear cessation, the signal fluctuations exhibit a very rapid slowing down, as can be observed in Fig. 4. Now, being  $I(t)$  not stationary for a time period long enough

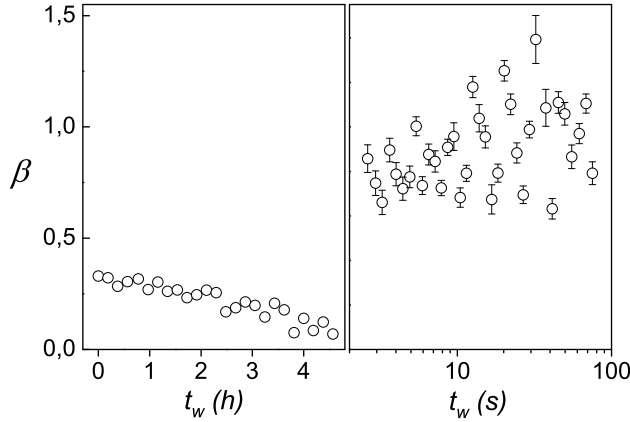


FIG. 2: Difference of the two aging regimes after shear rejuvenation as evidenced from the evolution of the  $\beta$  parameter, deduced from a stretched exponential fit  $\exp[-(t/\tau_s)^\beta]$  of the intensity autocorrelation function. *Left*: aging of a sample rejuvenated before entering the arrested phase. *Right*: aging of a rejuvenated gelled sample.

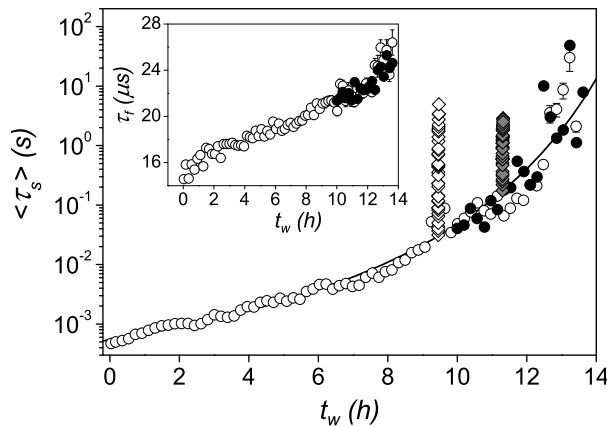


FIG. 3: Complete rejuvenation of the Laponite sample in the slow aging regime, *i.e.* before gelation. Average slow relaxation time  $\langle \tau_s \rangle$  is plotted as a function of waiting time  $t_w$  for a sample aging soon after filtration (empty circles) and for the same sample aging after the application of a shear rate of  $100 \text{ s}^{-1}$  for 2 minutes, 13.4 hours after filtration (full circles).  $t_w$  is shifted in order to superimpose the first  $\langle \tau_s \rangle$  measured after the application of shear with the first aging curve (empty circles). The black line is a guide for the eye. In the *inset* the fast relaxation time  $\tau_f$  is plotted as a function of  $t_w$  for the two aging evolution with the same shift in  $t_w$ . The slow aging regime is also compared to the fast aging regime, which is observed after the shear rejuvenation of a gelled sample: white diamonds represent the evolution of the slow relaxation time after a shear rate  $\dot{\gamma}_1 = 0.5 \text{ s}^{-1}$ , while grey diamonds are for  $\dot{\gamma}_1 = 100 \text{ s}^{-1}$ . Both curves are shifted in  $t_w$  through the procedure previously described.

to collect the data, the intensity correlation function cannot be obtained by time averaging and an ensemble averaging over many rejuvenating experiments is used:  $g^{(2)}(t_w, t) = \langle I(q, t_w) I(q, t_w + t) \rangle_e / \langle I(q, t_w) \rangle_e^2$ , where  $\langle \dots \rangle_e$  indicates the ensemble average over several intensity evolutions acquired after cessation of a repeated shear application. In particular, after the system has been left aging for 72 hours in order to reach gelation, a strong shear rate  $\dot{\gamma}_0$  is first applied in order to eliminate wall slip in the following shear application, then the system is sheared at a given  $\dot{\gamma}_1 < \dot{\gamma}_0$  for two minutes. After shear cessation the intensity fluctuations are collected for a time interval of two minutes with a time resolution of  $0.01 \text{ s}$ ; then a shear rate of the same value  $\dot{\gamma}_1$  is applied again for two minutes and the cycle starts again. The whole measurement lasts several hours and we obtain an ensemble of hundreds of acquisitions after the same initial conditions are imposed. In any acquisition, the intensity fluctuations look stationary in a log-linear plot of the intensity evolution, as shown in the bottom panel of Fig. 4. To speed up the computation of the correlation function, the acquired counts are thus logarithmically binned: a logarithmic binning of  $t_w$  is performed and the counts are averaged in each bin. The intensity autocorrelation function is then calculated as an ensemble average over all the bunches of counts, in the time window  $10^{-2} - 10^2$  for a set of waiting times between 1 and 40 s (Fig. 1, right frame). The time interval  $t_w < 1 \text{ s}$  is not considered, as the correlation functions may be influenced by inertial effects due to flow stop. In order to show that an aging of the sample under shear [21] is negligible during the whole experiment, we also calculate the correlation functions by taking only the first or last group of acquired counts and obtain the same results. The ensemble averaged correlation functions are first fitted by a stretched exponential decay, the fast component of dynamics being below the present time window. Results of the data analysis are checked to be invariant under different binning and fitting procedures. Compared to normal aging, the new aging regime entered by the rejuvenated gelled sample is characterized by correlation functions of a different form and by a much more rapid evolution of the slow relaxation time with  $t_w$ . In particular, the stretching parameter of the correlation function statistically fluctuates around one and doesn't seem to depend on the waiting time (Fig. 2, right panel). The correlation function can thus be well fitted by a single exponential decay. Besides, through the effect of the shear, the structural relaxation time soon after shear cessation is reduced by many orders of magnitude from the value characterizing the arrested phase, which must be higher than  $100 \text{ s}$  (Fig. 3). Then,  $\tau_s$  shows a power law dependence on  $t_w$ :  $\tau_s = A t_w^c$  (Fig. 5). To compare the fast aging evolution in this regime to the slow aging evolution characterizing the regime before gelation, we added in Fig. 3 the plot of the slow relaxation time evolution in this second regime, for the

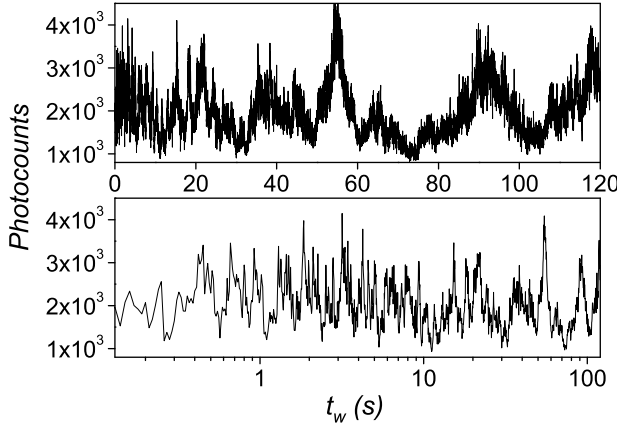


FIG. 4: Fast slowing down of the scattered intensity fluctuations with the waiting time for a rejuvenated gelled Laponite sample. *Top*: the evolution of the counts revealed by the photomultiplier in  $10^{-2}$  s soon after shear cessation is plotted,  $t_w = 0$  corresponds to the shear stop. *Bottom*: log-linear plot of the counts evolution; a logarithmic binning of  $t_w$  has been performed and the counts have been averaged in each bin.

applied stresses  $\dot{\gamma}_1 = 0.5, 100 \text{ s}^{-1}$ . A power law behavior of the structural relaxation time versus  $t_w$ , with exponent close to one, has already been observed after rejuvenation of aged samples through MS-DWS experiments on clay suspensions [10, 12] and on other colloidal glasses [9]. Also in normal aging, clay suspensions have shown such a power law behavior, but only for very long waiting times [20].

In order to investigate the power law behavior of the aging dynamics as a function of the shear rate value applied for rejuvenation, we repeated the same experiment by varying  $\dot{\gamma}_1$ . For small applied shear rates, Laponite aged samples exhibit a nonlinear velocity profile [25]. Heterodyne photocorrelation is thus used to measure the detailed velocity profile, in order to calculate  $\dot{\gamma}_1$  as the local shear rate in the scattering volume [13]. On the contrary, for higher applied shear, the shear rate is constant along the gap and  $\dot{\gamma}_1$  can simply be calculated as the cone velocity over the gap width. For  $\dot{\gamma}_1 \ll \dot{\gamma}_0$ , no significant changes are found in the  $c$  exponent of the power law. Indeed, for different values of  $\dot{\gamma}_1$ , spanning more than one decade:  $\dot{\gamma}_1 = 0.5, 3, 16 \text{ s}^{-1}$ , all the aging curves are well fitted by the power law with  $c$  lying in the interval  $1.23 \pm 0.08$  (Fig. 5). When  $\dot{\gamma}_1 = 70, 100 \text{ s}^{-1}$  instead, the  $c$  parameter drops to a value smaller than one and lies in the interval  $0.56 \pm 0.08$ . On the contrary, for all the shear rates here investigated, the  $A$  parameter increases with  $\dot{\gamma}_1$ , but it is not clear why the relaxation time soon after shear cessation is longer for an higher applied shear rate. In particular, one would expect that when the shear re-

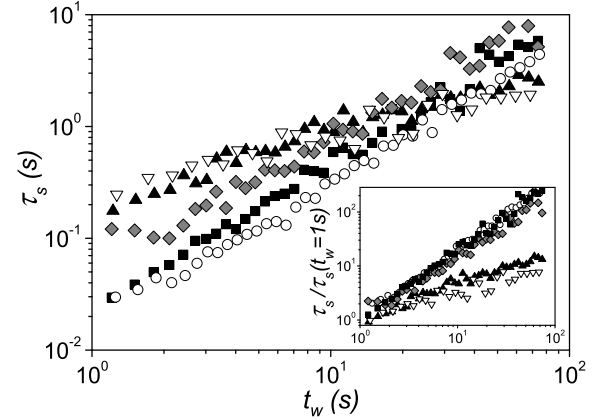


FIG. 5: Aging after rejuvenation of a gelled Laponite sample. The evolution with  $t_w$  of the slow relaxation time  $\tau_s$ , obtained from a single exponential fit of the intensity auto-correlation function, is plotted for various applied shear rates  $\dot{\gamma}_1$ . Circles:  $\dot{\gamma}_1 = 0.5 \text{ s}^{-1}$ , squares:  $\dot{\gamma}_1 = 3 \text{ s}^{-1}$ , diamonds:  $\dot{\gamma}_1 = 16 \text{ s}^{-1}$ , down-triangles:  $\dot{\gamma}_1 = 70 \text{ s}^{-1}$  and up-triangles:  $\dot{\gamma}_1 = 100 \text{ s}^{-1}$ . All the curves are well fitted by the power law  $\tau_s = A t_w^c$ . When small enough shear rates are applied ( $\dot{\gamma}_1 \ll 100 \text{ s}^{-1}$ ) the  $c$  exponent lies in the interval  $1.23 \pm 0.08$ . For higher shear rates ( $\dot{\gamma}_1 = 70, 100 \text{ s}^{-1}$ ), the  $c$  exponent drops to a value smaller than one, lying in the interval  $0.56 \pm 0.08$ . On the contrary, the  $A$  parameter increases with the shear rate for all the curves. In the inset,  $\tau_s / [\tau_s(t_w = 1 \text{ s})]$  is plotted as a function of  $t_w$  in order to better distinguish among the two groups of curves.

juvenation effect dominates aging, the inverse shear rate sets the slow relaxation timescale. However, in our data, we don't find this scaling for the slow relaxation time soon after shear cessation. For example, at small shear rates, the shear does accelerate the system dynamics, but the slow relaxation time gets much smaller than the inverse shear rate.

Finally, consistency with classical DLS has been checked for this original method of DLS employed to measure the intensity correlation function for a rapidly aging sample. In order to compare the correlation functions measured through both methods, we monitored the aging dynamics of a Laponite sample under shear at small  $t_w^0$ . In this regime, the system dynamics after shear cessation are stationary over the timescale of the tens of seconds and can thus be investigated through classical DLS also. Soon after cell loading, the sample is left aging under shear at  $\dot{\gamma} = 100 \text{ s}^{-1}$  and shear is stopped each 60 s, a pause of 5 s is taken in order to avoid inertial effects due to flow stop and then the scattered intensity is acquired for 1 s, with a time resolution of  $10^{-5}$  s. Each hour, the time-averaged intensity correlation function is also measured through classical DLS by stopping the shear for 80

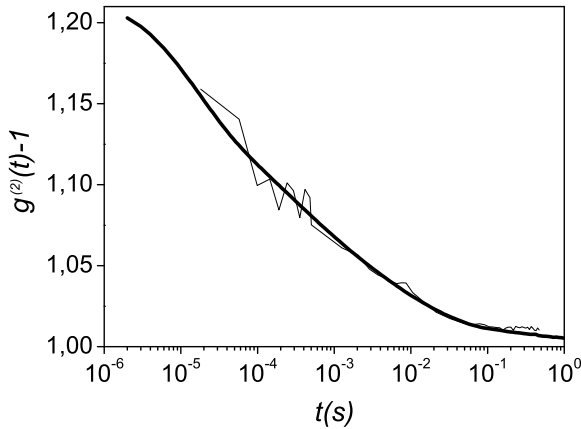


FIG. 6: Intensity correlation function measured as an ensemble average over many intensity acquisitions after shear cessation (thin line) compared to the time averaged correlation function measured through classical DLS (bold line). Measurements are performed on a Laponite sample aging under shear at  $\dot{\gamma} = 100 \text{ s}^{-1}$  for 24 h. As the sample ages during this long acquisition time, the correlation function plotted in bold line is an average of all the correlation functions acquired during the experiment through classical DLS.

s. The experiment lasts 24 h and the ensemble averaged intensity correlation function is calculated from all the acquired bunches of counts. Such a long acquisition time is necessary in order to reach a good statistics in the correlation function. In comparison to MS-DLS technique, where the intensity correlation function is calculated as an ensemble average over the speckle pattern, the acquisition time is extremely large, but the time resolution is much higher and enables the investigation of faster dynamics. As expected for this regime, the intensity correlation function is independent on  $t_w$ , the time elapsed since shear stop. On the contrary, as the system under shear keeps on aging with  $t_w^0$  [21], the dynamics change during the experiment and the ensemble averaged correlation function will provide an average value of the slow relaxation timescale. The ensemble averaged intensity correlation function is thus compared to the average of all the intensity correlation functions measured during the experiment through classical DLS (Fig. 6). In conclusion, intensity correlation function measured through an ensemble average over many acquisitions of the intensity evolution after shear cessation shows a good agreement with the one measured through classical DLS, where an average over the time origin is performed.

## CONCLUSIONS

We show the existence of two different regimes of aging for a suspension of charged discoidal clay particles after shear rejuvenation. Before gelation, classical DLS measurements have shown that a shear flow can completely rejuvenate the sample. The system dynamics after shear cessation depend on the applied shear rate and the following aging evolution is identical to the one after sample preparation: the fast relaxation time increases slightly with the waiting time  $t_w$ , while the slow relaxation time grows exponentially with  $t_w$  and becomes strongly stretched. On the contrary, in a gelled sample, aging dynamics after shear rejuvenation proceed very rapidly, so classical DLS measurements cannot be used and a novel dynamic light scattering method to measure the intensity correlation function has been proposed. An ensemble average over many rejuvenating experiments is used and the validity of this method is checked through comparison with classical DLS measurements. With this method, we investigated the aging dynamics of a gelled sample after shear rejuvenation by measuring the ensemble averaged intensity correlation function. Its time evolution is different from the one typical of the other regime, as its decay is characterized by a single exponential. Moreover, the slow relaxation time soon after shear stop is reduced by many orders of magnitude with respect to the large relaxation time typical of the arrested phase, while a very rapid evolution of the aging follows. In particular, we observed a power law behavior of the slow relaxation time with  $t_w$ , whose exponent shows two different values for small or high applied shear rates. Further studies are needed to clarify the nature of these different aging evolutions after shear rejuvenation and how they are linked to the gelation process.

The authors wish to thank Gianni Bolle and Md Islam Deen for technical assistance.

---

\* Electronic address: francesca.ianni@phys.uniroma1.it

- [1] P. Sollich, F. Lequeux, P. Hébraud, and M. E. Cates, Phys. Rev. Lett., **78**, 2020, (1997).
- [2] R. G. Larson, *The Structure and Rheology of Complex Fluids*, Oxford University Press (1999).
- [3] M. Fuchs and M. E. Cates, Phys. Rev. Lett. **89**, 248304 (2002).
- [4] L. Berthier, J.-L. Barrat, and J. Kurchan, Phys. Rev. E **61**, 5464-5472 (2000).
- [5] R. Yamamoto and A. Onuki J. Chem. Phys. **117**, 2359, (2002).
- [6] L. Berthier and J.-L. Barrat J. Chem. Phys. **116**, 6228, (2002).
- [7] L. Angelani, G. Ruocco, F. Sciortino, P. Tartaglia, and F. Zamponi, Phys. Rev. E **66**, 061505 (2002).
- [8] D. Bonn, S. Tanase, B. Abou, H. Tanaka, and J. Meunier, Phys. Rev. Lett., **89**, 015701, (2002).

- [9] V. Viasnoff and F. Lequeux, Phys. Rev. Lett. **89**, 065701 (2002).
- [10] F. Ozon, T. Narita, A. Knaebel, G. Debrégeas, P. Hébraud, J.-P. Munch, Phys. Rev. E, **68**, 032401, (2003).
- [11] G. Petekidis, A. Moussaïd, and P. N. Pusey, Phys. Rev. E **66**, 051402 (2002).
- [12] S. Kaloun, M. Skouri, A. Knaebel, J.-P. Münch, P. Hébraud, Phys. Rev. E **72**, 011401 (2005).
- [13] B. Berne and R. Pecora, Dynamic Light Scattering, Wiley, New York, (1976).
- [14] W. Götze and L. Sjögren, Phys. Rev. A **43**, 5442 (1991).
- [15] H. Van Olphen, *An Introduction to Clay Colloid Chemistry*, 2nd ed. (Wiley, New York, 1977).
- [16] M. Kroon, G. H. Wegdam, and R. Sprik, Phys. Rev. E, **54**, 6541, (1996).
- [17] B. Ruzicka, L. Zulian, G. Ruocco, Phys. Rev. Lett., **93**, 258301, (2004).
- [18] B. Ruzicka, L. Zulian, G. Ruocco, Langmuir, **22**, 1106, (2006).
- [19] B. Abou, D. Bonn, and J. Meunier, Phys. Rev. E, **64**, 021510, (2001).
- [20] M. Bellour, A. Knaebel, J. L. Harden, F. Lequeux, J.-P. Münch, Phys. Rev. E, **67**, 031405, (2003).
- [21] R. Di Leonardo, F. Ianni, and G. Ruocco, Phys. Rev. E, **71**, 011505, (2005).
- [22] R. Di Leonardo, S. Gentilini, F. Ianni, G. Ruocco J. non-Crystalline Solids, *to be published*.
- [23] The PhotonLab package is available for download at: <http://glass.phys.uniroma1.it/dileonardo/photonlab.html>.
- [24] R. Richert, J. Phys.: Condens. Matter **14**, R703 (2002).
- [25] D. Bonn, P. Coussot, H. T. Huynh, F. Bertrand, and G. Debrégeas, Europhys. Lett., **59**, 786, (2002).